$4b + X$ via electroweak multi-Higgs production as smoking gun signals for the Type-I 2HDM at the LHC

Prasenjit Sanyal

30, July 2024

Konkuk University, Korea

Outline and Reference

- QCD vs Electroweak (EW) production of multi-Higgs states in the context of Type-I 2HDM.
- Fermiophobic BSM Higgses, Higgs-gauge and Higgs-Higgs couplings in Type-I 2HDM.
- $4b + X$ final state at the LHC, mediated dominantly via EW processes.
- Reconstruction of the non-SM or BSM Higgs bosons.

PHYSICAL REVIEW LETTERS **131,** 231801 (2023)

Electroweak Multi-Higgs Production: A Smoking Gun for the Type-I Two-Higgs-Doublet Model

Tanmoy Mondal,[1,2,*] Stefano Moretti,[3,4,†] Shoaib Munir,[5,6,‡] and Prasenjit Sanyal[7,§]
[1]*Department of Physics, Osaka University, Toyonaka, Osaka 560-0043, Japan*
[2]*Birla Institute of Technology and Science, Pilani, 333031, Rajasthan, India*
[3]*School of Physics and Astronomy, University of Southampton, Southampton SO17 1BJ, United Kingdom*
[4]*Department of Physics and Astronomy, Uppsala University, Box 516, SE-751 20 Uppsala, Sweden*
[5]*East African Institute for Fundamental Research (ICTP-EAIFR), University of Rwanda, Kigali, Rwanda*
[6]*Department of Physics, Faculty of Natural Sciences and Mathematics, St. Olaf College, Northfield, Minnesota 55057, USA*
[7]*Department of Physics, Konkuk University, Seoul 05029, Republic of Korea*

QCD induced multi-Higgs production

(1) Pair of neutral scalars via gluon fusion:

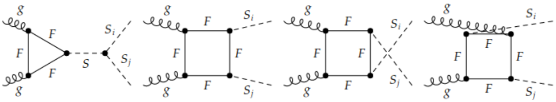

(2) $b\bar{b}$ annihilation to a pair of neutral scalars:

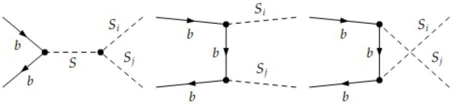

(3) $H^{\pm}$ pair creation via gluon fusion:

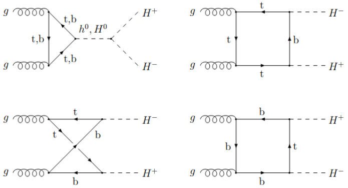

(4) $H^{\pm}$ pair creation $b\bar{b}$ annihilation:

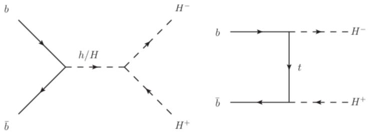

Electroweak multi-Higgs production

(1) Pair of neutral scalars:

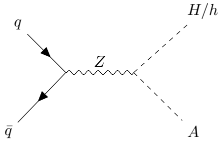

(2) $H^{\pm}$ pair creation:

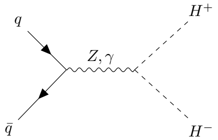

(3) Charged two body states:

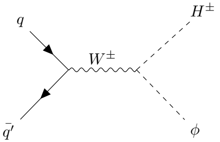

The charged two body states are not possible via QCD processes

QCD vs EW production of multi-Higgs states

Eur. Phys. J. C (2019) 79:512
https://doi.org/10.1140/epjc/s10052-019-7025-8

THE EUROPEAN PHYSICAL JOURNAL C

Regular Article - Theoretical Physics

Electroweak production of multiple (pseudo)scalars in the 2HDM

Rikard Enberg[1,a], **William Klemm**[1,2,b], **Stefano Moretti**[3,c], **Shoaib Munir**[4,5,d]

[1] Department of Physics and Astronomy, Uppsala University, Box 516, 751 20 Uppsala, Sweden
[2] School of Physics and Astronomy, University of Manchester, Manchester M13 9PL, UK
[3] School of Physics and Astronomy, University of Southampton, Southampton SO17 1BJ, UK
[4] School of Physics, Korea Institute for Advanced Study, Seoul 130-722, Republic of Korea
[5] East African Institute for Fundamental Research (ICTP-EAIFR), University of Rwanda, Kigali, Rwanda

Parameter scans:

m_H : 150 − 750 GeV; $m_{H\pm}$: 50 − 750 GeV; $m_A = 50 - 750$ GeV
$\sin(\beta - \alpha)$: −1.0 − 1.0; m_{12}^2 : $0 - m_A^2 \sin\beta\cos\beta$; $\tan\beta$: 2 − 25.

Cross sections at 13 TeV for charged two body states

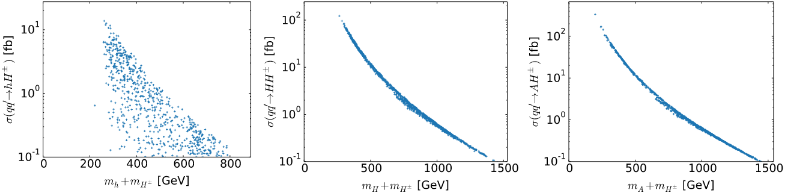

Cross sections at 13 TeV for charged three body states

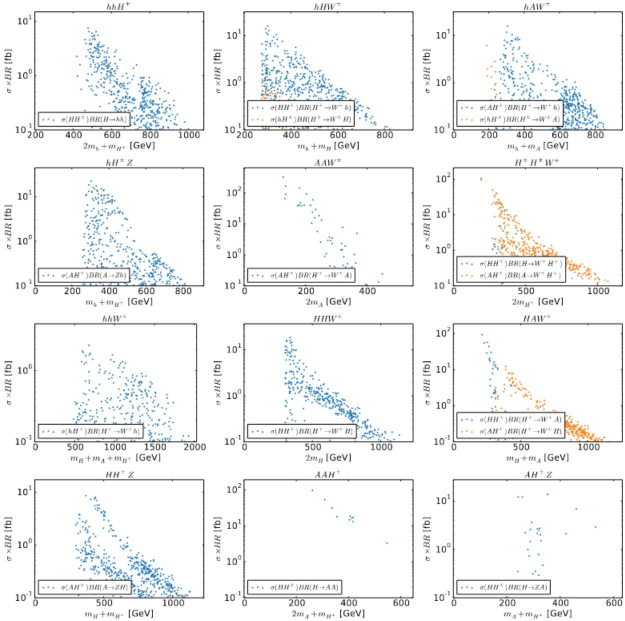

Cross sections at 13 TeV for neutral two body states

Neutral two body states have contributions from QCD as well as EW processes.

(A) Two body states where EW processes dominate the combined gg and $b\bar{b}$ QCD processes:

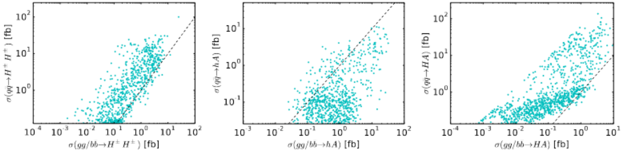

(B) Two body states where combined gg and $b\bar{b}$ QCD processes dominate the EW processes:

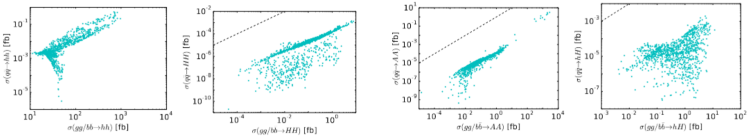

Cross sections at 13 TeV for neutral three body states

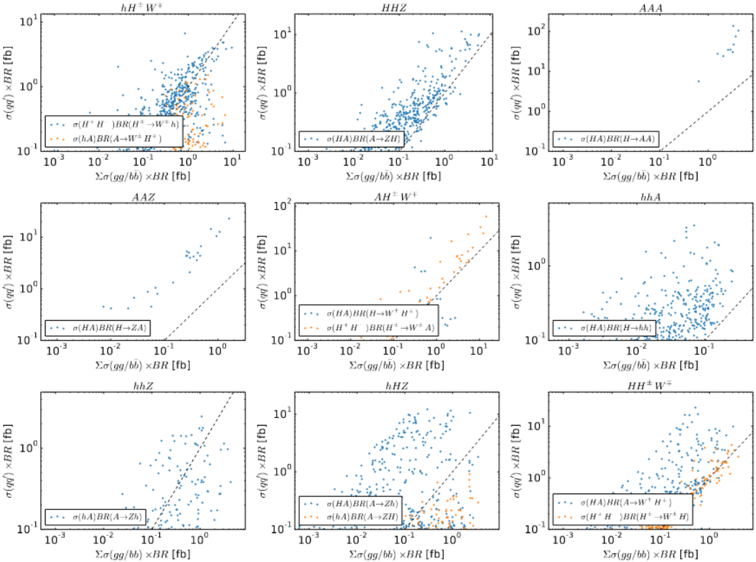

Major Findings

(A) EW production of neutral multi-Higgs states can dominate over the QCD induced production in Type-I 2HDM. **Reason: Fermiophobic nature of the BSM Higgs bosons.**

(B) EW productions are more complete as they can provide charged two body states.

(C) EW processes are ideal to probe the various Higgs-Higgs couplings appearing in 2HDM potential as well as the Higgs-gauge couplings.

Overview of Type I 2HDM

- The scalar sector of 2HDM consists of two $SU(2)$ doublets Φ_i, $i = 1,\ 2$.

$$\mathcal{V}_{\text{2HDM}} = -m_{11}^2\Phi_1^\dagger\Phi_1 - -m_{22}^2\Phi_2^\dagger\Phi_2 - \left[m_{12}^2\Phi_1^\dagger\Phi_2 + \text{h.c.}\right] + \frac{1}{2}\lambda_1\left(\Phi_1^\dagger\Phi_1\right)^2 + \frac{1}{2}\lambda_2\left(\Phi_2^\dagger\Phi_2\right)^2 + \lambda_3\left(\Phi_1^\dagger\Phi_1\right)\left(\Phi_2^\dagger\Phi_2\right) + \lambda_4\left(\Phi_1^\dagger\Phi_2\right)\left(\Phi_2^\dagger\Phi_1\right) + \left[\frac{1}{2}\lambda_5\left(\Phi_1^\dagger\Phi_2\right)^2 + \text{h.c.}\right]$$

- After EWSB the two $SU(2)$ Higgs doublets can be written as:

$$\Phi_i = \begin{pmatrix} \phi_i^+ \\ \frac{v_i+\rho_i+i\eta_i}{\sqrt{2}} \end{pmatrix}, \qquad v_i = \langle\rho_i\rangle \quad v = \sqrt{v_1^2+v_2^2} = 246\ \text{GeV}, \qquad \tan\beta = v_2/v_1.$$

- Scalar spectrum: Two *CP* even Higgses (h and H), a pseudoscalar (A) and a pair of charged Higgs ($H^\pm$).

- Alignment limit: $\sin(\beta-\alpha) \to 1$ implies that the couplings of h is like SM Higgs boson.

- $H,\ A$ and $H^\pm$ can be termed as the non-SM or BSM Higgs bosons.

- In Type-I 2HDM, all the fermions are coupled to the second Higgs doublet, Φ_2.

- After the EWSB the Yukawa Lagrangian in terms of the mass eigenstates:

$$
\begin{aligned}
\mathcal{L}^{\rm 2HDM}_{\rm Yuk,\ I} &= -\sum_{f=u,d,\ell} \frac{m_f}{v}\left(\xi^f_h \bar{f} h f + \xi^f_H \bar{f} H f - i\xi^f_A \bar{f}\gamma_5 A f\right) \\
&- \left\{ \frac{\sqrt{2}V_{ud}}{v}\bar{u}\left(\xi^u_A m_u P_L + \xi^d_A m_d P_R\right) H^+ d + \frac{\sqrt{2}m_l}{v}\xi^l_A \bar{\nu}_L H^+ l_R + \text{h.c.}\right\}
\end{aligned}
$$

ξ^u_h	ξ^d_h	ξ^ℓ_h	ξ^u_H	ξ^d_H	ξ^ℓ_H	ξ^u_A	ξ^d_A	ξ^ℓ_A
c_α/s_β	c_α/s_β	c_α/s_β	s_α/s_β	s_α/s_β	s_α/s_β	$\cot\beta$	$-\cot\beta$	$-\cot\beta$

- $\xi^f_A \propto 1/\tan\beta \Longrightarrow$ **fermiophobic *A*, $H^\pm$** for $\tan\beta \gg 1$.
  $\xi^f_H = s_\alpha/s_\beta = c_{\beta-\alpha} - s_{\beta-\alpha}/\tan\beta \Longrightarrow$ **fermiophobic *H*** for $\tan\beta \gg 1$, $\sin(\beta-\alpha) \to 1$.

Higgs-gauge couplings

CP conserving 2HDM:

(A) hVV : $\sin(\beta-\alpha)h^{\rm SM}_{hVV}$ $\quad$ HVV : $\cos(\beta-\alpha)h^{\rm SM}_{hVV}$ $\quad$ AVV : 0 $\quad$ $V=Z, W^\pm$

(B) hAZ_μ : $\frac{g}{2c_{\theta_W}}\cos(\beta-\alpha)(p_h-p_A)_\mu$ $\quad$ HAZ_μ : $-\frac{g}{2c_{\theta_W}}\sin(\beta-\alpha)(p_H-p_A)_\mu$

(C) $H^\mp W^\pm h$: $\mp\frac{ig}{2}\cos(\beta-\alpha)(p_h-p_{H^\pm})_\mu$ $\quad$ $H^\mp W^\pm h$: $\pm\frac{ig}{2}\sin(\beta-\alpha)(p_H-p_{H^\pm})_\mu$
$H^\mp W^\pm A$: $\frac{g}{2}(p_A-p_{H^\pm})_\mu$

Higgs-Higgs couplings

CP conserving 2HDM: λ_{hhh}, λ_{hhH}, λ_{hHH}, λ_{HHH}, λ_{hAA}, λ_{HAA}, $\lambda_{hH^+H^-}$, $\lambda_{HH^+H^-}$

(A) $\lambda_{hAA}=\frac{1}{4vs_\beta c_\beta}\left\{(4M^2-2m_A^2-3m_h^2)c_{\alpha+\beta}+(2m_A^2-m_h^2)c_{\alpha-3\beta}\right\}$, $\quad M^2=m_{12}^2/s_\beta c_\beta$
$\lambda_{hAA}=\frac{1}{v}(2M^2-2m_A^2-m_h^2)$, $\quad$ for $\sin(\beta-\alpha)\to 1$

(B) $\lambda_{Hhh}=\frac{1}{2vc_\beta s_\beta}c_{\beta-\alpha}\left\{(3M^2-2m_h^2-m_H^2)s_{2\alpha}-M^2s_{2\beta}\right\}$
$\lambda_{Hhh}=0$, $\quad$ for $\sin(\beta-\alpha)\to 1$

(C) $\lambda_{HAA}=\frac{1}{4vs_\beta c_\beta}\left\{(4M^2-2m_A^2-3m_H^2)s_{\alpha+\beta}-(m_H^2-2m_A^2)s_{\alpha-3\beta}\right\}$
$\lambda_{HAA}=\frac{2}{vt_{2\beta}}(m_H^2-M^2)$, $\quad$ for $\sin(\beta-\alpha)\to 1$

Limits: (1) Theoretical (2) EWPOs (3) $B \to X_s\gamma$ (4) Collider constraints

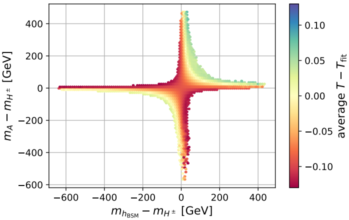

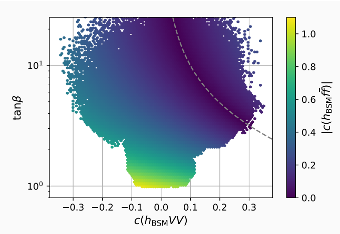

Henning Bahl, Tim Stefaniak, Jonas Wittbrodt, JHEP 06 (2021), 183

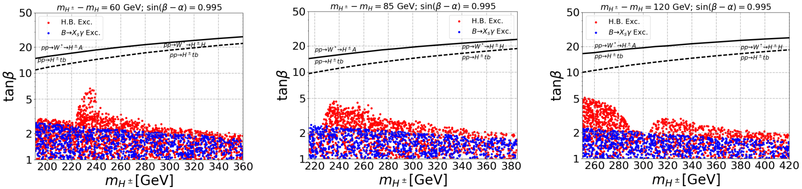

Tanmoy Mondal, Prasenjit. Sanyal, JHEP 05 (2022) 040

$4b + X$ via EW processes

EW processes contributing to the $4b + X$ mode:

$$q\bar{q}' \begin{cases} 1.\ AAW:\ pp \to H^{\pm}A \to [AW][A] \to 4b + X \\ 2.\ AAAW:\ pp \to H^{\pm}H \to [AW][AA] \to 4b + X \\ 3.\ AAZW:\ pp \to H^{\pm}H \to [AW][AZ] \to 4b + X \end{cases}$$

$$q\bar{q} \begin{cases} 4.\ AAA:\ pp \to HA \to [AA][A] \to 4b + X \\ 5.\ AAZ:\ pp \to HA \to [AZ][A] \to 4b + X \\ 6.\ AAWW:\ pp \to H^{+}H^{-} \to [AW][AW] \to 4b + X \end{cases}$$

Benchmark Points:

BP	m_A [GeV]	$m_{H^{\pm}}$ [GeV]	m_H [GeV]	$\tan\beta$	$\sin(\beta-\alpha)$	m_{12}^2 [GeV^2]	BR($H \to AA$)	BR($H \to AZ$)
1	70	169.7	144.7	7.47	0.988	2355.0	0.99	0.006
2	50	169.8	150.0	17.11	0.975	1275.0	0.48	0.505

Cross sections at $\sqrt{s} = 13$ TeV:

BP	AAW [fb]	$AAAW$ [fb]	$AAZW$ [fb]	AAA [fb]	AAZ [fb]	$AAWW$ [fb]
1	142.3	79.7	0.35	171.6	0.76	25.2
2	198.0	37.1	29.0	101.3	79.3	27.7

Background: QCD multi-jet = 9×10^6 pb and $t\bar{t}$ + jets = 834pb.

Stefano Moretti, Shoaib Munir, Tanmoy Mondal and Prasenjit Sanyal, Phys.Rev.Lett(2023)

Pseudoscalar mass reconstruction

(1) b-jets ≥ 4, $p_T > 20$ GeV, $|\eta| < 2.5$

(2) Three possible combinations of two b-jet pairs out of four leading b-jets: (a,b; c,d), (a,c; b,d) and (a,d; b,c).

(3) The combination which minimizes

$$\Delta R = |(\Delta R_1 - 0.8)| + |(\Delta R_2 - 0.8)|$$

is selected, where

$$\Delta R_1 = \sqrt{(\eta_a - \eta_b)^2 + (\phi_a - \phi_b)^2}$$
$$\Delta R_2 = \sqrt{(\eta_c - \eta_d)^2 + (\phi_c - \phi_d)^2}$$

(4) After b-jet pairing, we impose assymmetry cut

$$\alpha = \frac{|m_1 - m_2|}{m_1 + m_2} < 0.2$$

m_1 and m_2 are the invariant masses of two b-jet pairs.

BP1

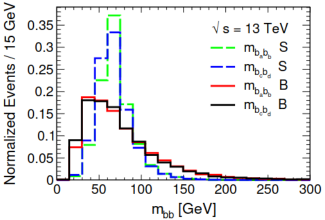

BP2

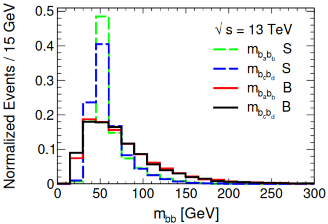

***Sanyal, et al.*, Phys.Rev.Lett(2023)**

Charged Higgs mass reconstruction

$H^{\pm}$ reconstruction based on the *AAW* topology

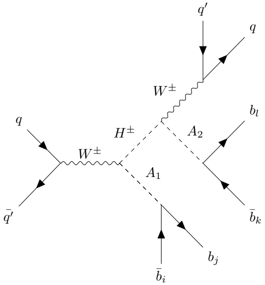

BP1

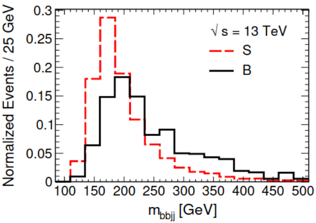

(1) b-jets ≥ 4 and jets ≥ 2 such that $j\,j \in X$ $(q\bar{q}' \rightarrow A_1 H^{\pm} \rightarrow A_1 A_2 W \rightarrow 4b + j\,j)$.

(2) Leading two jets satisfy $m_{jj} = m_W \pm 25$ GeV.

(3) The combination of two b-jet pairs with invariant mass within 45 GeV window around m_A and satisfying the assymmetry cut is selected.

(4) Prompt pseudoscalar: A_1, non-prompt pseudoscalar: A_2. Then $p_T(A_1) > p_T(A_2)$.

(5) If $b_i b_j$ is from A_1 and $b_k b_l$ is from A_2. Then $(p_i + p_j)_T > (p_k + p_l)_T$.

(6) $b_k b_l$ and the jet pair make the four jet system. The invariant mass of $b_k b_l jj$ reconstructs the mass of $H^{\pm}$.

(7) If more than one combination of four jet system is possible. The correct combination gives the maximum separation of the reconstructed $H^{\pm}$ and A_1 in the $\eta - \phi$ space.

Sanyal, et al., Phys.Rev.Lett(2023)

Heavy Higgs mass reconstruction

H reconstruction based on the AAA topology

(1) b-jets ≥ 6 ($q\bar{q} \to A_1 H \to A_1 A_2 A_3 \to 6b$)

(2) The combination of three b-jet pairs with invariant mass within 45 GeV window around m_A and satisfying the assymmetry cut is selected.

(3) Prompt pseudoscalar: A_1, non-prompt pseudoscalar: $A_{2,3}$ Then $p_T(A_1) > p_T(A_{2,3})$

(4) If $b_i b_j$ is from A_1, then $(p_i + p_j)_T > (p_k + p_l)_T$ and $(p_i + p_j)_T > (p_m + p_n)_T$.

(5) $b_k b_l$ and $b_m b_n$ make the $4b$-jet system. The invariant mass of the $4b$-jet system reconstructs the mass of H.

(6) If more than one combination of $4b$-jet system is possible. The correct combination gives the maximum separation of the reconstructed H and A_1 in the $\eta - \phi$ space.

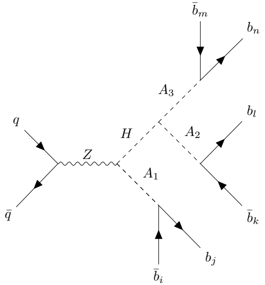

BP1

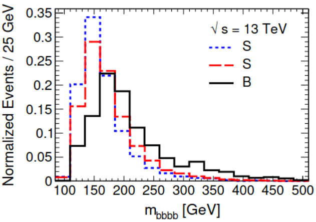

Sanyal, et al., Phys.Rev.Lett(2023)

Hurdles of H reconstruction:

(1) $6b$-jet events are very rare. Events with $5b$ jets are considered and the 6^{th} b-jet is assumed to be one of the light jets.

(2) The reconstruction starts to fail if $H \to AZ$ dominates over $H \to AA$ decay.

	Reconstructed Higgs bosons at 3000 fb^{-1}								
	A			$H^{\pm}$			H		
BP	σ_S [fb]	σ_B [fb]	$\frac{S}{\sqrt{B}}$	σ_S [fb]	σ_B [fb]	$\frac{S}{\sqrt{B}}$	σ_S [fb]	σ_B [fb]	$\frac{S}{\sqrt{B}}$
1	15.4	8864	8.9σ	2.22	482	5.5σ	2.55	309	7.9σ
2	10.4	10175	5.7σ	1.33	491	3.3σ	1.06	256	3.6σ

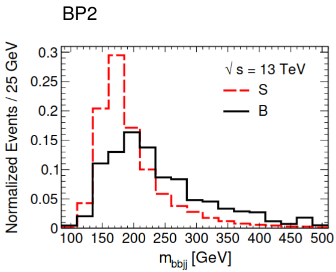

Sanyal, et al., Phys.Rev.Lett(2023)

Conclusions

- In a fermiophobic BSM framework like Type-I 2HDM, the EW induced multi-Higgs production dominates over the QCD induced processes.
- EW processes provides the charged two body states which complement the QCD processes.
- $4b + X$ final state obtained through EW processes is useful to reconstruct the masses of all the BSM Higgses.
- Reconstruction of the BSM Higgses serves as probes for the non-SM Higgs-Higgs and Higgs-gauge couplings.

Conclusions

- In a fermiophobic BSM framework like Type-I 2HDM, the EW induced multi-Higgs production dominates over the QCD induced processes.
- EW processes provides the charged two body states which complement the QCD processes.
- $4b + X$ final state obtained through EW processes is useful to reconstruct the masses of all the BSM Higgses.
- Reconstruction of the BSM Higgses serves as probes for the non-SM Higgs-Higgs and Higgs-gauge couplings.

THANK YOU!

Backup: *b*-(miss)tagging efficiencies

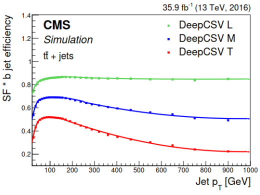

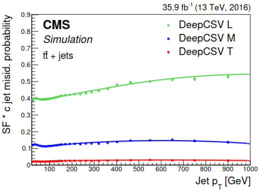

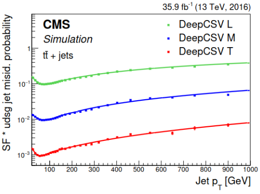

Table 6: Polynomial functions used to fit the efficiency of the three working points of the DeepCSV algorithm for the three jet flavours as a function of the jet p_T for jets with $20 < p_T < 1000$ GeV.

Flavour	Working point	p_T (GeV)	Function
b	DeepCSV L	20–160	$0.4344 + 0.02069p_T - 0.0004429{p_T}^2 + 5.137 \times 10^{-6}{p_T}^3 - 3.406 \times 10^{-8}{p_T}^4 + 1.285 \times 10^{-10}{p_T}^5$ $-2.559 \times 10^{-13}{p_T}^6 + 2.084 \times 10^{-16}{p_T}^7$
		160–300	$0.714 + 0.002617p_T - 1.656 \times 10^{-5}{p_T}^2 + 4.767 \times 10^{-8}{p_T}^3 - 6.431 \times 10^{-11}{p_T}^4 + 3.287 \times 10^{-14}{p_T}^5$
		300–1000	$0.872 - 6.885 \times 10^{-5}p_T + 4.34 \times 10^{-8}{p_T}^2$
	DeepCSV M	20–50	$0.194 + 0.0211p_T - 0.000348{p_T}^2 + 2.761 \times 10^{-6}{p_T}^3 - 1.044 \times 10^{-8}{p_T}^4 + 1.499 \times 10^{-11}{p_T}^5$
		50–250	$0.557 + 0.003417p_T - 3.26 \times 10^{-5}{p_T}^2 + 1.506 \times 10^{-7}{p_T}^3 - 3.63 \times 10^{-10}{p_T}^4 + 3.522 \times 10^{-13}{p_T}^5$
		250–1000	$0.768 - 0.00055p_T + 2.876 \times 10^{-7}{p_T}^2$
	DeepCSV T	20–50	$-0.033 + 0.0225p_T - 0.00035{p_T}^2 + 2.586 \times 10^{-6}{p_T}^3 - 9.096 \times 10^{-9}{p_T}^4 + 1.212 \times 10^{-11}{p_T}^5$
		50–160	$0.169 + 0.013p_T - 0.00019{p_T}^2 + 1.373 \times 10^{-6}{p_T}^3 - 4.923 \times 10^{-9}{p_T}^4 + 6.87 \times 10^{-12}{p_T}^5$
		160–1000	$0.62 - 0.00083p_T + 4.3078 \times 10^{-7}{p_T}^2$
c	DeepCSV L	20–300	$0.398 - 0.000182p_T + 2.53 \times 10^{-6}{p_T}^2 - 6.796 \times 10^{-9}{p_T}^3 + 8.66 \times 10^{-12}{p_T}^4 - 4.42 \times 10^{-15}{p_T}^5$
		300–1000	$0.35 + 0.000374p_T - 1.81 \times 10^{-7}{p_T}^2$
	DeepCSV M	20–200	$0.136 - 0.000639p_T + 6.188 \times 10^{-6}{p_T}^2 - 2.26 \times 10^{-8}{p_T}^3 + 3.61 \times 10^{-11}{p_T}^4 + 2.09 \times 10^{-14}{p_T}^5$
		200–1000	$0.103 + 0.00014p_T - 1.15 \times 10^{-7}{p_T}^2$
	DeepCSV T	20–65	$0.0234 - 8.417 \times 10^{-5}p_T + 1.24 \times 10^{-6}{p_T}^2 - 5.5 \times 10^{-9}{p_T}^3 + 9.96 \times 10^{-12}{p_T}^4 - 6.32 \times 10^{-15}{p_T}^5$
		165–1000	$0.0218 + 2.46 \times 10^{-5}p_T - 2.021 \times 10^{-8}{p_T}^2$
udsg	DeepCSV L	20–150	$0.245 - 0.0054p_T + 6.92 \times 10^{-5}{p_T}^2 - 3.89 \times 10^{-7}{p_T}^3 + 1.021 \times 10^{-9}{p_T}^4 - 1.007 \times 10^{-12}{p_T}^5$
		150–1000	$0.0558 + 0.000428p_T - 1.0 \times 10^{-7}{p_T}^2$
	DeepCSV M	20–225	$0.019 - 0.00031p_T + 3.39 \times 10^{-6}{p_T}^2 - 1.47 \times 10^{-8}{p_T}^3 + 2.92 \times 10^{-11}{p_T}^4 - 2.12 \times 10^{-14}{p_T}^5$
		225–1000	$0.00328 + 5.7 \times 10^{-5}p_T + 4.7 \times 10^{-9}{p_T}^2$
	DeepCSV T	20–150	$0.00284 - 8.63 \times 10^{-5}p_T + 1.38 \times 10^{-6}{p_T}^2 - 9.69 \times 10^{-9}{p_T}^3 + 3.19 \times 10^{-11}{p_T}^4 - 3.97 \times 10^{-14}{p_T}^5$
		150–1000	$0.00063 + 4.51 \times 10^{-6}p_T + 2.83 \times 10^{-9}{p_T}^2$

CMS Collaboration, arXiv:1712.07158